Large supercooled liquid region and phase separation in the Zr–Ti–Ni–Cu–Be bulk metallic glasses

C. C. Hays,[a] C. P. Kim, and W. L. Johnson
W. M. Keck Laboratory of Engineering Materials, 138-78 California Institute of Technology, Pasadena, California 91125

(Received 30 April 1999; accepted for publication 29 June 1999)

Results of calorimetric, differential thermal analysis, and structural measurements are presented for a series of bulk metallic glass forming compositions in the Zr–Ti–Cu–Ni–Be alloy system. The calorimetric data for five alloys, prepared along the tie line between phase separating and nonphase separating compositions, show that the transition from phase separating to nonphase separating behavior is smooth. The bulk glasses near the center of the tie line exhibit large supercooled liquid regions: $\Delta T \approx 135$ K, the largest known for a bulk metallic glass. © *1999 American Institute of Physics.* [S0003-6951(99)01734-9]

There are a number of multicomponent bulk metallic glass (BMG) forming alloy systems, e.g., La–Ni–Al,[1] Zr–Al–Cu–Ni,[2] Zr–Ti–Cu–Ni–Be,[3] and Zr–Ti–Cu–Ni.[4] The Be-containing bulk glass $Zr_{41.2}Ti_{13.8}Cu_{12.5}Ni_{10}Be_{22.5}$ (Vit 1) exhibits an exceptional glass forming ability (GFA) and thermal stability with respect to crystallization. The liquid-state viscosity of the Be-BMG alloys is ≈ two orders of magnitude higher than in pure metals or alloys, typically $\eta(\text{Be-BMG}) \approx 5$ poise.[5] The high melt viscosities of the Be-BMG compositions yield very sluggish crystallization kinetics in the supercooled liquid region (SLR). The crystallization behavior of Vit 1 has been determined by electrostatic levitation (ESL) and calorimetric methods.[6,7] These results, when combined with the results of small angle neutron scattering (SANS) measurements conducted by Schneider, Johnson, and Thiyagarajan show that primary crystallization is preceded by phase separation in the SLR.[8] This phase separation process shows many of the features of a spinodal decomposition, with a spinodal temperature of ≈ 671 K. The decomposition process is followed by the nucleation of fcc nanocrystals on a length scale correlated with the spinodal wavelength, $\lambda_s \approx 14$ nm. The bulk glass $Zr_{46.75}Ti_{8.25}Cu_{7.5}Ni_{10}Be_{27.5}$ (Vit 4) also exhibits an excellent GFA. This alloy exhibits little phase separation prior to crystallization. To elucidate this behavior, results of thermophysical property measurements are presented for compositions along the tie line between the compositions of Vit 1 and Vit 4, the phase separating and nonphase separating alloys, respectively. The thermophysical property data show that through controlled changes in alloy composition the GFA may be altered drastically. The experimental data are related to the known features of the Vit 1 time-temperature-transformation (TTT) diagram determined from the ESL measurements.

The details of the methods used to prepare the master alloys are described elsewhere.[9] The tie-line alloy compositions were prepared in the form of thin strips, $1 \times 5 \times \approx 25$ mm (thickness by width by length), by injection casting into a Cu metal mold. The specimen compositions prepared along the tie line from Vit 1 to Vit 4, labeled Vit 1, 1(a), 1(b), 1(c), and 4, respectively, are presented in Table I. The nominal compositions are used in this letter. The strategy employed in this alloy series involves incrementally changing the Zr/Ti, Cu/Ni, and Be ratios in a smooth fashion.

Figure 1 shows the results of differential scanning calorimetry (DSC) measurements conducted on portions of the 1 mm injection cast strips. The data for each composition are shifted along the heat flow axis by successive increments of −2.5 W/g. The DSC traces show a smooth evolution of the thermal properties on going along the tie line from alloys 1 to 4. The data for Vit 1, the uppermost shown in Fig. 1, exhibits the characteristic behavior for this composition. This behavior is manifest by a distinct endothermal heat effect due to the glass transition followed by three characteristic steps of heat release upon crystallization of the metastable supercooled liquid.[7] The inset to the figure shows the glass transition region with expanded scaling. The first exothermic peak we attribute to phase separation and primary crystallization. The second and third exothermic peaks are thought to be due to secondary crystallization and the formation of high temperature crystalline phases, respectively. The second alloy of the series, Vit 1(a), shows the first exothermic peak reduced in magnitude and shifted to a higher temperature, indicating a decomposition similar to that observed in Vit 1 prior to primary crystallization. This slight exothermic effect is attributed to the growth of primary nanocrystals prior to the crystallization of the remaining matrix. The calorimetric data for Vit 1(a) closely resemble the DSC data for Vit 1 specimens annealed in the SLR at a temperature $T = 643$ K, for 6000 s.[7] The DSC traces for alloys 1(b) and 1(c) do not exhibit any indication of decomposition in the SLR prior to

TABLE I. Vit 1–Vit 4 tie-line compositions.

Alloy	Alloy composition
1	$(Zr_{75}Ti_{25})_{55}(Ni_{45}Cu_{55})_{22.5}Be_{22.5}$
1(a)	$(Zr_{77.5}Ti_{22.5})_{55}(Ni_{48}Cu_{52})_{21.25}Be_{23.75}$
1(b)	$(Zr_{80}Ti_{20})_{55}(Ni_{51}Cu_{49})_{20}Be_{25}$
1(c)	$(Zr_{82.5}Ti_{17.5})_{55}(Ni_{54}Cu_{46})_{18.75}Be_{26.25}$
4	$(Zr_{85}Ti_{15})_{55}(Ni_{57}Cu_{43})_{17.5}Be_{27.5}$

[a]Electronic mail: chays@hyperfine.caltech.edu

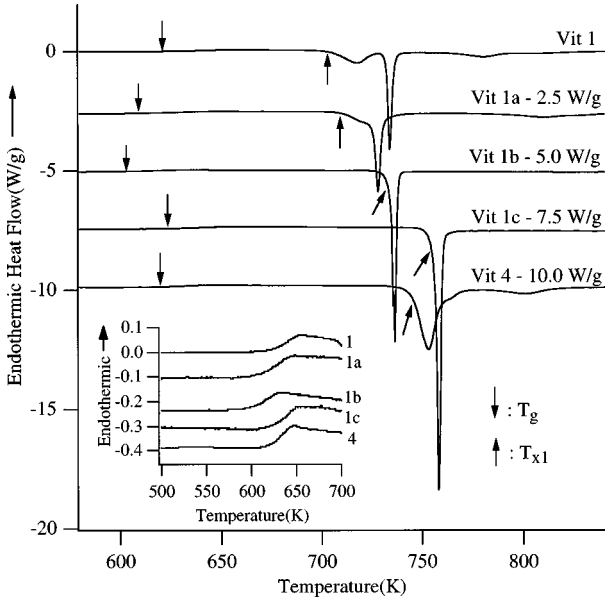

FIG. 1. DSC data for Vit 1–Vit 4 tie-line compositions.

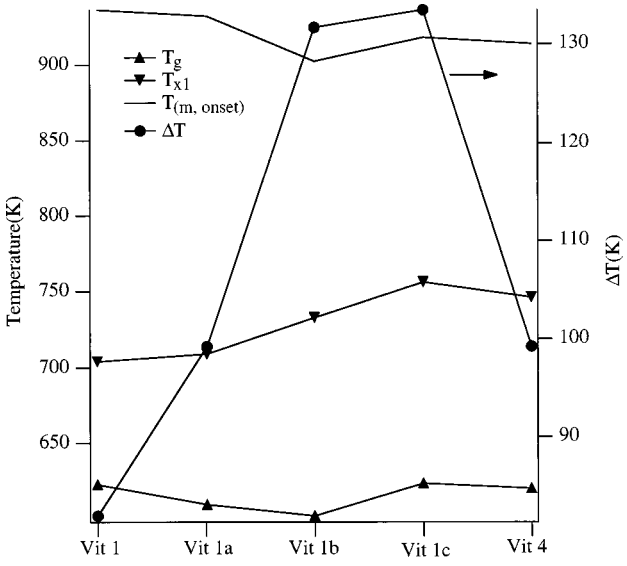

FIG. 2. DSC and DTA results for the Vit 1–Vit 4 tie-line compositions.

primary crystallization. Instead, the latter two alloys demonstrate a ''eutectic-like'' primary crystallization event, where the various crystalline phases are simultaneously formed upon primary crystallization. This was confirmed by the x-ray diffraction (XRD) measurements conducted on the DSC specimens following heating to 853 K; the XRD patterns showed lines characteristic of a number of crystalline phases commonly observed in crystalline Zr–Ti–Cu–Ni–Be specimens, e.g., the Ti_2Ni or Zr_2Cu (''E93'' or ''$MoSi_2$'' structure types), Cu_2TiZr or Ti_2Cu ($MoSi_2$ structure type), NiTiZr [$MgZn_2$ (Laves phase)] structure types.[9] The absence of high temperature exothermic reactions in the DSC traces for alloys 1(b) and 1(c) also further supports this point.

The width of the SLR for Vit 1(c), $\Delta T=(T_x-T_g)\approx 135\,\mathrm{K}$, shows that this composition may be a highly processable bulk glass, with a correspondingly low critical cooling rate. The magnitude of this ΔT value is the largest known value for a bulk metallic glass, surpassing the ΔT value reported for ''fluxed'' $Pd_{40}Cu_{30}Ni_{10}P_{20}$ specimens, which have a critical cooling rate of less than 1 K/s.[10] The DSC trace for the Vit 4 composition begins to display a high temperature shoulder beyond the primary crystallization event, indicating that a small degree of phase separation may occur in this alloy. This is supported by unpublished three-point beam bending viscosity measurements conducted on Vit 4 by Waniuk.[11] The DSC results, together with the results of differential thermal analysis (DTA) scans are graphically summarized in Fig. 2 for the tie-line alloys. Figure 2 shows that the onset temperature of primary crystallization, T_{x1}, rapidly increases on going along the tie line from alloy 1 to 1(c). The onset of melting, T_{onset}, for the two alloys, 1(b) and 1(c), is low, and both demonstrate a near eutectic DTA trace, with a narrow melting interval. The respective values for the 1(b) and 1(c) compositions are $T_{\mathrm{onset}}[1(b)]=903\,\mathrm{K}$ and $T_{\mathrm{onset}}[1(c)]=918\,\mathrm{K}$. Both are less than the melting point of pure aluminum (933 K). The reduced glass transition temperature, given by the ratio of the glass transition temperature to the melting temperature, for the Vit 1(c) composition is $T_{\mathrm{rg}}=0.68$. This value is well above $T_{\mathrm{rg}}=2/3$, which in the Turnbull model marks the point where the probability of nucleating crystals in the undercooled liquid becomes vanishingly small.[12]

The implications of the exceptional GFA of the Vit 1(b) and Vit 1(c) bulk glasses are readily described by reference to the TTT diagram (see Fig. 3) of Vit 1.[13] The Vit 1 TTT diagram is a superposition of high and low temperature curves, a feature also observed in undercooling experiments conducted in graphite crucibles.[14] Figure 3 also shows the temperature-time, (T_{x1},t), (data marked as: ○) data for the onset of primary crystallization, T_{x1}, as measured in the DSC and presented in Fig. 1 for the Vit 1–Vit 4 tie-line compositions. The onset temperatures for primary crystallization recorded on heating in a calorimetric measurement generally lie well below the corresponding values measured via the containerless ESL method. This can be attributed to the growth rate and relative stability of the crystalline phases

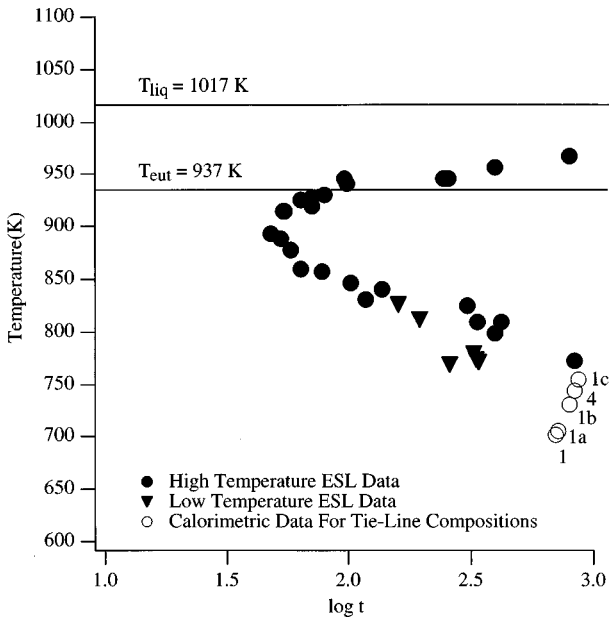

FIG. 3. Experimental Vit 1 TTT diagram, and Vit 1–Vit 4 tie-line calorimetric data.

nucleated on cooling versus heating. The calorimetric data reflect the increasing T_{x1} values for the alloy series; 1, 1(a), 1(b), 1(c), and 4. Note that the Vit 1(c) data point, ○ 1(c), lies uppermost for the four alloys. Schematically drawn lower branches are left off the figure for clarity. The calorimetric (T_{x1},t) data points show that the overall features of the TTT diagram for the Vit 1(c) alloy are sharpened, meaning that (1) the Vit 1(c) nose temperature may be pushed back to longer times or (2) the lower branch of the Vit 1(c) TTT diagram is effectively raised or erased. Considering only the relative shift of the nose temperature, we calculate a maximum shift to larger times, of $\delta t_{1c}(\text{nose}) \approx 1.2\,\text{s}$ for Vit 1(c), a negligible quantity. The temperature shift, $\Delta T_x = T_{x1}[1(c)] - T_{x1}(1) = 757 - 704\,\text{K} = 53\,\text{K}$, effectively removes the low temperature ESL data points from the TTT diagram. Thus, the competing crystalline phases responsible for the high temperature portion of the TTT diagram are unaffected by the change in composition on going along the tie line. However, the change in composition is quite effective in increasing the overall processability of the glass forming liquid. The ''hypothetical'' Vit 1(c) TTT diagram has a nose temperature similar in magnitude to the Vit 1 composition. Thus, the critical cooling rate for Vit 1(c) is probably near ≈ 2 K/s, i.e., the cooling rate just has to pass this nose of the TTT diagram at $t_c \approx 48$ s. However, the removal of the lower branch of the TTT diagram will greatly increase the GFA and processability of the glass, as the nucleation of the low temperature crystalline phases is appropriately ''frustrated'' by the alloy composition. This is manifest experimentally in the preparation of the Vit 1(c) master alloy. Master 25 g rods of Vit 1(c) have consistently exhibited an x-ray diffraction pattern absent of any Bragg peaks, and the thin crystalline skull (≈ 1 mm thick) present on the bottom of as-cast Vit 1 rods is reduced in thickness or absent.

The calorimetric results for the alloys that lie along the tie line from Vit 1 to Vit 4 show the dramatic influence of composition on these alloys' thermophysical properties. It has been proposed that the spinodal decomposition observed in Vit 1 may result in the formation of coexisting strong and fragile liquids in the SLR.[7] The BMG composition Vit 1(c) exhibits what appears to be strong liquid behavior. The data presented show that the composition manifold of the Zr–Ti–Cu–Ni–Be system is complex, as revealed by the dramatic changes in thermophysical behavior for small changes in composition.

The authors would like to acknowledge the support of the U.S. Department of Energy (Grant No. DEFG-03-86ER45242). One of us (C. C. Hays) would like to acknowledge fruitful discussions with Ulrich Geyer and T. A. Waniuk during the preparation of this manuscript. The authors would also like to thank John Haygarth of Teledyne Wah-Chang Inc. for providing the crystal bar Ti and Zr used in the preparation of these alloys.

[1] A. Inoue, T. Zhang, and T. Masumoto, Mater. Trans., JIM **31**, 425 (1990).
[2] A. Inoue, T. Zhang, N. Nishiyama, K. Ohba, and T. Masumoto, Mater. Trans., JIM **33**, 937 (1992).
[3] A. Peker and W. L. Johnson, Appl. Phys. Lett. **63**, 2342 (1993).
[4] X. H. Lin and W. L. Johnson, J. Appl. Phys. **78**, 6514 (1995).
[5] R. Busch, A. Masuhr, E. Bakke, and W. L. Johnson, Mater. Sci. Forum **269–272**, 547 (1998).
[6] Y. J. Kim, R. Busch, W. L. Johnson, A. J. Rulison, and W. K. Rhim, Appl. Phys. Lett. **65**, 2136 (1994).
[7] T. A. Waniuk, R. Busch, A. Masuhr, and W. L. Johnson, Acta Mater. **46**, 5229 (1998).
[8] S. Schneider, W. L. Johnson, and P. Thiyagarajan, Appl. Phys. Lett. **68**, 493 (1996).
[9] C. C. Hays, P. Kim, and W. L. Johnson, Mater. Res. Soc. Sym. Proc. **554** (in press).
[10] N. Nishiyama and A. Inoue, Acta Mater. **47**, 1487 (1999).
[11] Unpublished work of T. A. Waniuk, California Institute of Technology, 1999.
[12] D. Turnbull and M. H. Cohen, Nature (London) **189**, 131 (1961); D. Turnbull, Contemp. Phys. **10**, 473 (1969).
[13] Y. J. Kim, R. Busch, W. L. Johnson, A. J. Rulison, and W. K. Rhim, Appl. Phys. Lett. **68**, 1057 (1996).
[14] J. Schroers, R. Busch, A. Masuhr, and W. L. Johnson, J. Non-Cryst. Solids (to be published).